IEEE Access
Multidisciplinary | Rapid Review | Open Access Journal

Received January 11, 2018, accepted February 28, 2018, date of publication May 4, 2018, date of current version May 24, 2018.

Digital Object Identifier 10.1109/ACCESS.2018.2822051

A Novel Control Algorithm for DC Motors Supplied by PVs Using Fuzzy Cognitive Networks

THODORIS L. KOTTAS, (Student Member, IEEE),
ATHANASIOS D. KARLIS, (Senior Member, IEEE),
AND YIANNIS S. BOUTALIS, (Member, IEEE)
Department of Electrical and Computer Engineering, Democritus University of Thrace, 67100 Xanthi, Greece
Corresponding author: Thodoris L. Kottas (tkottas@teiwm.gr)

ABSTRACT Photovoltaic (PV) arrays present non-linear I–V curves, which strongly depend on ambient temperature and solar insolation. This fact poses a problem in identifying the maximum PV power point. In this paper, a dc motor is powered by a PV array and an attempt is made to optimize the use of the PV energy while the DC motor is supplied with suitable current and voltage in order to match its load–speed characteristics. This is achieved through a dc/dc converter controlled by a fuzzy cognitive network (FCN), in parallel with an energy storage device (battery), so that the PV energy is always fully exploitable. The algorithm method uses an FCN and a fuzzy controller, which recognize the maximum power of the PV array very fast while at the same time, they control the speed of the dc motor, under different insolation and temperature conditions. The proposed algorithm is validated through the simulation studies and is proven to be effective.

INDEX TERMS Photovoltaic power systems, dc motors speed control, fuzzy systems, fuzzy cognitive networks.

I. INTRODUCTION

Photovoltaic (PV) energy turns out to be a promising substitute for conventional sources due to the growing demand on electricity, as it is an endless source of energy. The efficiency of power conversion from solar to electricity is low (around 15-20%). This is mainly due to the following reason; the power output of solar cells mainly depends on solar insolation and ambient temperature. Improving the efficiency of a photovoltaic system is achieved by finding the maximum operating point of the photovoltaic at any insolation and temperature levels.

In a PV array, solar energy is converted to electrical, which, in turn, could be used to directly supply DC loads, or might be stored in batteries or even supply AC loads with the use of a DC-AC inverter. In case of using a DC motor as a load connected to a PV array, the solar energy is converted into electrical and through the DC motor into mechanical. Alghuwainem [1], [2] attempted to match the characteristics of the DC motor to those of the photovoltaic, so that the system's performance would increase and the conversion of electrical energy to mechanical would have minimum losses.

The system in [1] consists of the PV array and the DC motor. Each one of the devices is characterized by its own different operating characteristics where there is only one operating point, depending on insolation and temperature, that corresponds to both which in turn defines the optimal operating non-linear point of the combined PV array – DC motor system. Each solar insolation level defines a unique PV array operating point, where power output reaches a maximum value. Since the maximum power point depends on solar insolation and temperature, it is difficult to reach the maximum efficiency of the PV array at all insolation levels. A review of studies referring to directly connected PV arrays with DC motors is made in [3], where it seems that the optimal operating point of DC motors is different from the maximum-power point of the connected PV arrays at various insolation levels, thus affecting negatively the efficiency of the PV array-DC motor system.

By using an electronic maximum power point tracking device, known as MPPT, the problem can be solved. MPPT constantly tracks, for certain temperature and radiation values, the appropriate I-V points of the PV array that produce the maximum power, and at the same time tries to match the pertinent I-V characteristic of the DC motor - through a DC/DC converter - so that motor rotates at the optimal – for each mechanical load - speed. By carefully selecting the

2169-3536 © 2018 IEEE. Translations and content mining are permitted for academic research only.
Personal use is also permitted, but republication/redistribution requires IEEE permission.
See http://www.ieee.org/publications_standards/publications/rights/index.html for more information.

characteristics of the DC motor so that they match the maximum power curve of the photovoltaic generator, an efficient operation can be achieved, but, according to [4] it does not apply to all levels of solar radiation. Dileep and Singh [5] conclude their selection criteria by saying that a non-isolated DC/DC converter plays an important role on the performance of a PV water pumping system, while others in [6] study the maximum mechanical energy produced by a DC motor when it is directly connected to a PV array. The researchers in [7] study the function of the mechanical loads fed by one or more independent PV arrays. An experimental comparison between two different PV installation techniques, i.e. a directly coupled PV - DC motor system and a system employing a constant voltage MPPT controller, is made in [8].

Other research efforts focus on the effectiveness and the advantages of connecting a Brushless DC Motor to a PV array. In [9], where a Zeta Converter, fed from a PV array, is used to drive a BLDC motor, authors proposed an incremental conductance MPPT algorithm, which offers soft starting of the motor. Sashidhar and Fernandes [10] compare induction motors with BLDC motors fed from PV arrays and show the effectiveness of BLDC motors, where experimental results of a motor prototype are presented. A single stage BLDC motor fed by a PV array through a voltage source inverter is presented in [11], where authors claim that this power conversion stage is simple and cost effective compared to other PV-DC motor drives.

Zinger and Braunstein [12] achieved to track the maximum power operating point of a PV array by discretely interchanging the series-parallel connections of solar cells, while other MPPT methods use either a normal mode of a DC-DC converter as presented by Schoeman and Van Wyk [13], or a step-up mode as in [14]. A comparison between various incremental conductance MPPT techniques, which in general showed a very good performance, especially at low solar insolation levels, is presented in [15], where authors investigate the drawbacks and the advantages of each technique.

A number of computational methods for the MPPT technique using fuzzy logic have been presented in the literature. Karthika *et al.* [16] use an interleaved boost converter, which is preferred due to high voltage gain from PV arrays, having a SiC MOSFET driver and a Fuzzy Logic MPPT Controller in order to adjust the speed of a DC motor, while a computational method based on fuzzy logic [17], [18] showed very good adaptation abilities under different solar insolation levels. An algorithm that does not require temperature and radiation measurement has shown very good MPPT matching in [19].

Matsukawa *et al.* [20] and Masoum *et al.* [21] introduced methods regarding the dynamic behavior of a PV array in order to study its interaction with the relevant MPPT system, while other researchers in [22] presented a new MPPT method using FCN with a Fuzzy Controller to track Maximum Power from a PV connected to any load. The same authors continued their research in [23] presenting the adaptation capability of the FCNs when dealing with the dynamic behavior a PV array or with the change of basic characteristics due to failures or degradation.

This paper presents a novel algorithm and a new topology evolving an MPPT controller, which uses Fuzzy Cognitive Networks (FCNs) and Fuzzy Sets theory. The FCN presented in this paper, is designed so that it can corporate with a Fuzzy Controller [10], which is used in parallel with the FCN to track the maximum power operation point of the PV array, supplying at the same time a DC shunt motor drive, by forcing it to operate at its optimal speed. FCNs presented in [22]–[24] introduced a complete computational and storage structure that enables the use of FCNs when there is a physical system needing description.

The paper is organized as follows: in Section 2 mathematical equations for an equivalent PV array are given in order to simulate the operation of a PV array under different meteorological data. In Section 3 the equations describing the steady state operation of the DC motor are also given while in Section 4 the fuzzy logic MPPT method is presented. Section 5 presents the converters and the new installation topology between the PV array and the DC motor using a battery for storing the extra power extracted from the PV. In Section 6 a brief introduction in Fuzzy Cognitive Networks is made and the graph of the proposed FCN is presented. Simulation results, of a commercially available PV array and a DC motor, are given in section 7. Conclusions are given in Section 8.

II. SIMULATION OF A PV ARRAY

The circuit, which is depicted in (Fig. 1), of a solar cell [25] is described by the following equations:

$$I_i = I_p - \left(I_{rr} \left(\frac{T}{T_r} \right)^3 e^{\frac{1.115}{k'A}\left(\frac{1}{T_r} - \frac{1}{T}\right)} \right) (e^{\frac{qV_i}{kTA}} - 1) - \frac{V_i}{R_{sh}} \tag{1}$$

$$I_{ph} = (I_{rr} + k_i(T - T_r))\frac{s}{100} mW/cm^2 \tag{2}$$

$$V_{oc} = \frac{AkT}{q} \ln \left(\frac{I_p}{I_{rr} \left(\frac{T}{T_r} \right)^3 e^{\frac{1.115}{k'A}\left(\frac{1}{T_r} - \frac{1}{T}\right)}} + 1 \right) \tag{3}$$

$$I_{rr} = \frac{(I_{scr} + k_i(T - T_r))\frac{s}{100}}{e^{\frac{V_{oc}q}{AkT}} - 1} \left[\left(\frac{T_r}{T} \right)^3 e^{-\frac{1.115}{k'A}\left(\frac{1}{T_r} - \frac{1}{T}\right)} \right] \tag{4}$$

$$R_{sh} = \frac{V_{oc}}{-\left(I_{rr} \left(\frac{T}{T_r} \right)^3 e^{\frac{1.115}{k'A}\left(\frac{1}{T_r} - \frac{1}{T}\right)} \right) (e^{\frac{qV_{oc}}{kTA}} - 1)} \tag{5}$$

where I_i and V_i are the output current and voltage respectively, q is the electron charge, k is Boltzmann's constant in J/K, k' is the same constant but in eV/K, k_i is a coefficient in A/K relating the short circuit current and temperature, A is the p–n junction ideality factor and is equal to 1.3 for Si-mono PV arrays, T is the cell temperature in Kelvin, T_r is the cell reference temperature at 25°C, I_{rr} is the reverse saturation

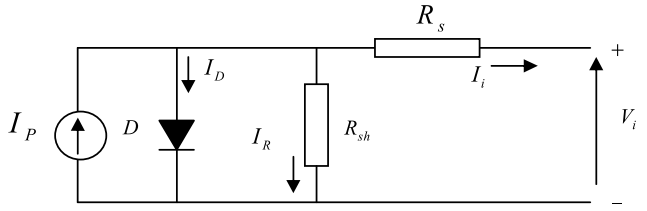

FIGURE 1. Equivalent circuit of a solar cell.

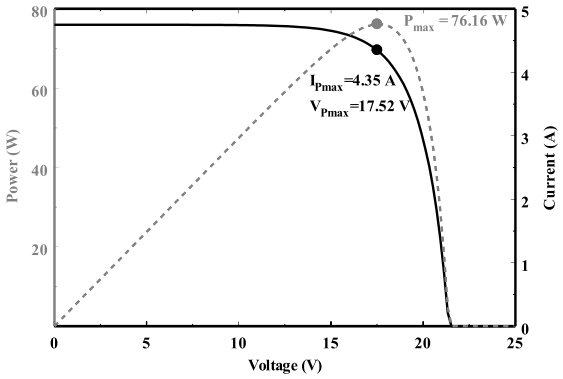

FIGURE 2. Current vs Voltage and Power vs Voltage diagram of a common PV array ($S = 100mW/cm^2$ and $T_r = 25°C$).

current at T_r, I_p is the photocurrent, I_{scr} is the short circuit current of the PV array at the cell reference temperature and insolation level S, The required data for eqs 1-5 are k_i, V_{oc}, I_{scr}, V_i, I_i, all given by the PV manufacturer at $T_r = 25°C$ and $S = 100mW/cm^2$.

A PV array is a non-linear current generator, which under constant insolation has an I–V characteristic diagram shown in Fig. 2. Fig. 3 shows I–V curves under different solar insolation levels, but at constant temperature.

For the case study, a PV array having $k_i = 2.8\ mA/°C$, $V_{oc} = 21.4\ V, I_{scr} = 4.48\ A, V_i = 17.52\ V$ and $I_i = 4.35\ A$, at $T_r = 25°C$ and $S = 100mW/cm^2$ is used.

III. MOTOR CHARACTERISTICS

The DC motor used in this study is a shunt DC motor with the following parameters:

Rated voltage	$V_{in} = 48$ V
Rated current	$I_{in} = 0.9$ A
Rated speed	$\omega = 45$ rad/sec
Armature resistance	$R_A = 0.5\ \Omega$
Mutual Inductance	$L_{AF} = 1.2$ H
Rated Load torque	$T_L = 0.001\omega^{1.8}$ Nm.

Iron and motor rotational losses are neglected

The motor voltage at steady state operation and the electromagnetic torque are:

$$V_{in} = \frac{T_L\omega + R_A\,(I_{in})^2}{I_{in}} \tag{6}$$

Fig. 4 shows motor Voltage and Speed versus current.

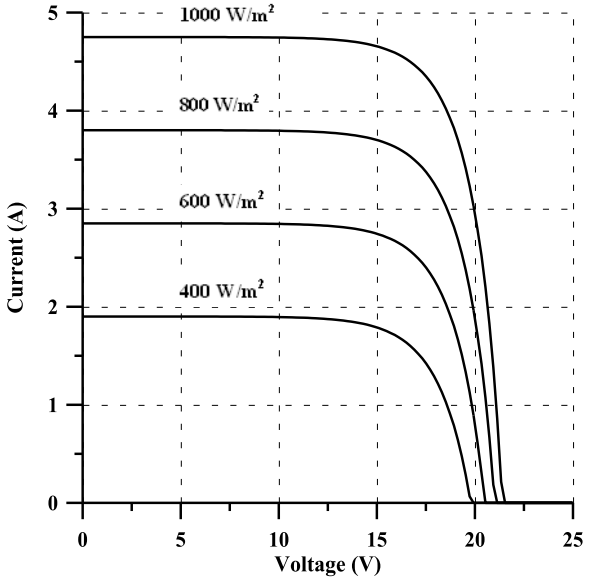

FIGURE 3. Current vs Voltage diagram of a common PV array at different insolation levels and steady temperature 25°C.

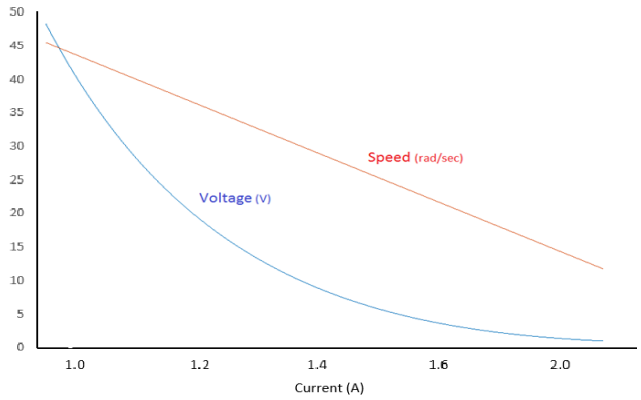

FIGURE 4. Current vs Voltage and Speed vs Voltage diagrams of a DC motor.

IV. PV - MOTOR-BATTERIES CIRCUIT

The main circuit components shown in Fig. 5 are a PV array, the shunt motor drive and a battery of 24V and 72Ah capacity. All components are interconnected through three buck boost DC/DC converters which have the following characteristics:

- Buck-boost converter input voltage: 0 to 74.1 V
- Buck-boost converter output voltage: 0 to 74.1 V
- switching frequency (fs) of transistor S: 33kHz

The driver circuit controls the power transistor S which is turned on and off with a rated duty ratio. The operation of buck-boost converters is given in [2].

For the buck-boost converter No1 using the transistor S1 the duty ratio $r1$ is related to the PV output Voltage and DC motor input Voltage through:

$$r1 = V_{in}/\,(V_{PV} + V_{in}) \tag{7}$$

where $r1$ is the duty ratio of the transistor S1 applied to converter No1.

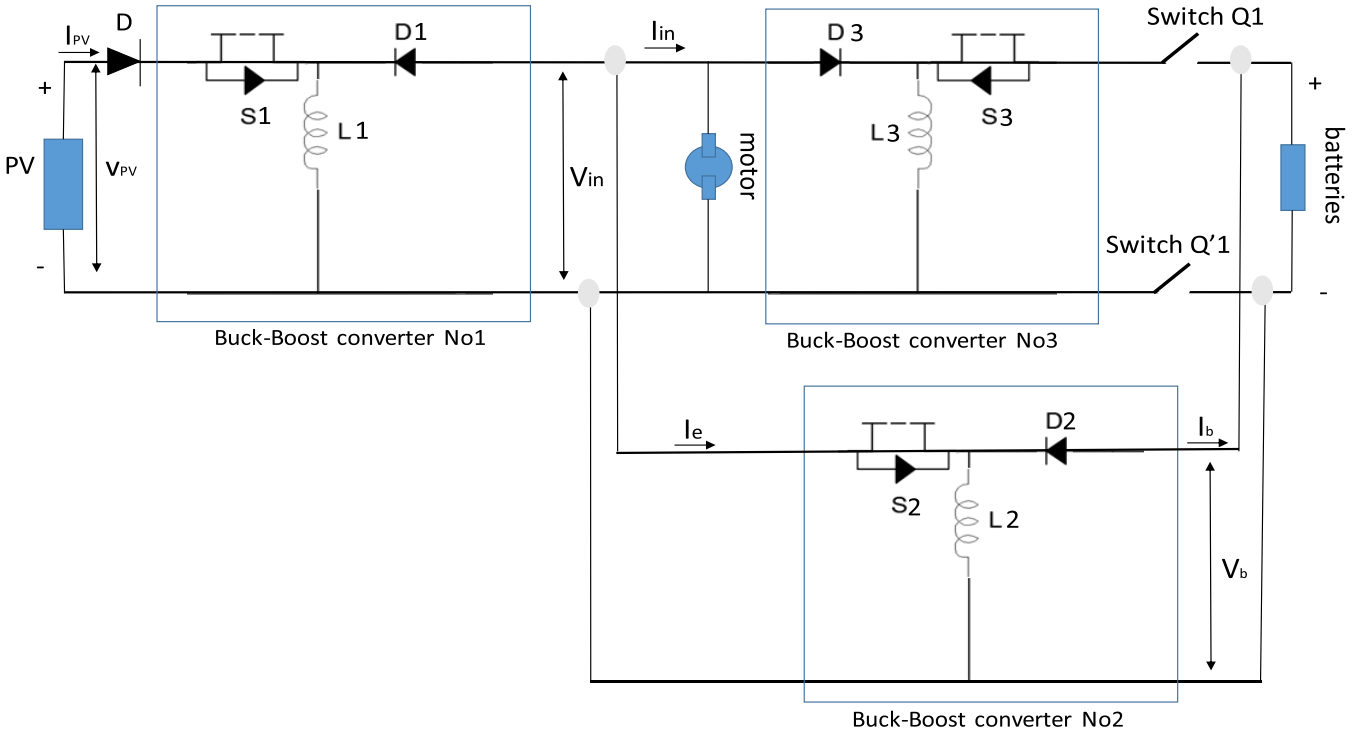

FIGURE 5. Topology of the system under study.

For the buck-boost converter No2 using the transistor S2 the duty ratio $r2$ is related to the Battery Voltage and DC motor input Voltage through:

$$r2 = V_b / (V_{in} + V_b) \tag{8}$$

For the converter No3 using the transistor S3 the duty ratio $r3$ is related to the DC motor input Voltage and Battery Voltage through:

$$r3 = V_{in} / (V_b + V_{in}) \tag{9}$$

Batteries in Fig. 5 are used to store the surplus energy from the PV array that is not applied to the motor, thus the algorithm is always tracking the maximum power extracted from the PV. The current I_e which is the input of converter No2 is equal to $I_e = (P_{PV} - P_{in}) / V_{in}$. When $V_{in}I_{in} > V_{PV}I_{PV}$ then switches $Q1$ and $Q'1$ are both closed and transistor S2 is always off with $V_b = 24Volt$. The transistor S3 is now in conducting mode in order to transfer the power from the batteries to the motor, while at the same time converter No2 is no longer transferring power from the PV to batteries. When $V_{in}I_{in} < V_{PV}I_{PV}$ then switches $Q1$ and $Q'1$ are both open and transistor S2 is in conducting mode, thus transferring power from PV to batteries.

V. SPEED CONTROL AND MAXIMUM POWER OPERATION POINT USING FUZZY LOGIC CONTROLLER [17]

The objective of the controller is to monitor the maximum power point of the PV array and at the same time to determine the correct value for the motor speed. As mentioned in the previous section, the optimum operating point of a PV array is determined by the values of solar insolation and temperature. To adjust and achieve this MPP value, a DC/DC converter is used between the load we want to supply and the PV array. By using the DC/DC converter we will be able to adjust the PV array output power and the input power of the motor so that the second rotates to the desired values.

A. FUZZIFICATION

In order to achieve the control, Won *et al.* [17] created a controller with two inputs on the left hand side part and a single output on the right hand side part of the fuzzy controller, where one of the inputs is the error E while the second one is the change of error CE at a sampling time k and they are given by the following equations:

$$E(k) = \frac{P_{PV}(k) - P_{PV}(k-1)}{I_{PV}(k) - I_{PV}(k-1)} \tag{10}$$

$$CE(k) = E(k) - E(k-1) \tag{11}$$

where $P_{PV}(k)$ and $I_{PV}(k)$ are the power and the current of the PV array. The controller continuously changes the P_{PV} value, by changing the duty ratio dr of the transistor S, which interrupts the values of the output voltage V_{PV} and current I_{PV}. At each iteration k, where the $P_{PV}(k)$ value is continuously changed, a correction in the duty ratio dr is performed in order to assure that the desired speed of the motor is achieved. The correction of duty ratio $r1$ is performed according to: $r1 = 1 - \left(V_{in}^{des} / V_{PV}(k)\right)$, where V_{in}^{des} is the desired motor voltage calculated by eq. (6) and $V_{PV}(k)$ is the PV array

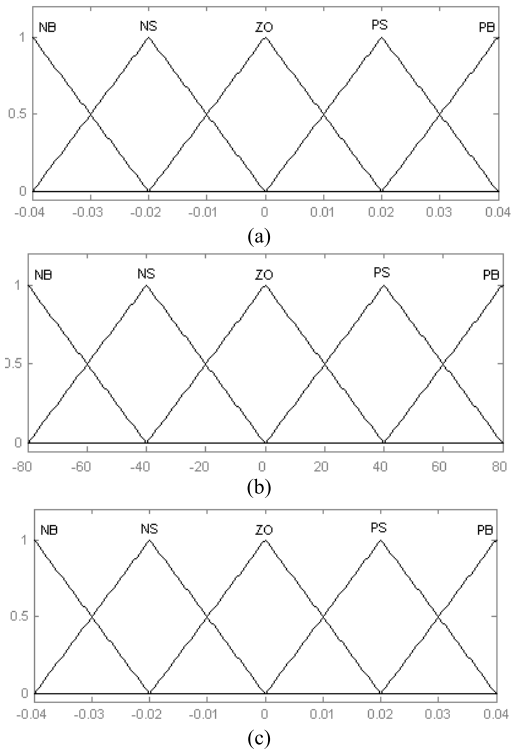

FIGURE 6. Triangular membership function for fuzzy. (a) input $E(k)$ (b) input $CE(k)$ (c) output dr.

voltage applied in time k from the controller. At iteration $k+1$, controller is checking whether the previous power value in iteration k is greater than the next value at iteration $k+1$, and the process is interrupted. If the $P_{PV}(k+1)$ is lower, the process is repeated until $E(k+1)=0$, where the maximum power point of the PV array is the value $P_{PV}(k)$. The fuzzy membership functions of sets $E(k)$ and $CE(k)$ are shown in figs 6a and 6b respectively. Fig. 6c shows the Finally Fig. 6c shows the membership functions of output set dr, how the on/off duty ratio $r1$ of the DC/DC converters transistor S1 varies.

B. INFERENCE METHOD

The rule table of the fuzzy controller, presented in Table 1, depicts the fuzzy interconnection between the fuzzy sets of $E(k)$, $CE(k)$ and duty ratio dr. The control rule is designed so that the input variable $E(k)$ must always be equal to zero.

An example control rule is:

IF $E(k)$ is PS AND $CE(k)$ is NB **THEN** dr is PS

As a fuzzy inference method we use the Mamdani's one including max-min operation fuzzy combination law. The Center of Area (COA) and the Max Criterion Method (MCM) are implemented for defuzzification purposes [26].

VI. THE FUZZY COGNITIVE NETWORK APPROACH FOR THE DC MOTOR – PV ARRAY SYSTEM

In this section an FCN is designed to represent the operation of a DC motor powered from a PV array. Our aim is to use the FCN, for estimating the Maximum Power Point of the PV array and in the same time to adjust the motor speed.

TABLE 1. Fuzzy rule table.

FUZZY SETS for output dr		CE(k)				
		NB	NS	ZO	PS	PB
E(k)	NB	ZO	ZO	NB	NB	NB
	NS	ZO	ZO	NS	NS	NS
	ZO	NS	ZO	ZO	ZO	PS
	PS	PS	PS	PS	ZO	ZO
	PB	PB	PB	PB	ZO	ZO

A. FCNs

Fuzzy Cognitive Networks were designed to be a methodology for modeling physical systems using the theories of both fuzzy logic and neural networks.

A graphical representation of FCN [27] is depicted in Fig. 7, where each node C1...C8 represents a characteristic of a physical system. For each node a characteristic number A_i is corresponding, representing its value which was evaluated after the real value of the system's variable was transformed. Vector A represents the values of the nodes in the interval [0,1] as follows:

$$A = \begin{bmatrix} A_1 & A_2 & A_3 & A_4 & A_5 & A_6 & A_7 & A_8 \end{bmatrix}^T$$

Between nodes exists a causality named "weights" and range in the interval $[-1,1]$. Weights map the cause-effect relationship between the nodes of the FCN. The value of each weight w_{ij} indicates how strongly concept (node) C_j influences concept C_i, i.e. an increase in the value of node C_j with a weight value of $w_{ij} > 0$ is translated as an increase in the value of node C_i. Otherwise, the value of the node C_j decreases if the value of w_{ij} is negative.

Matrix W of the aforementioned weights, referring to the FCN presented in Fig. 7, is given by:

$$W = \begin{bmatrix} 1 & w_{12} & w_{13} & w_{14} & 0 & w_{16} & 0 & 0 \\ w_{21} & 1 & 0 & 0 & 0 & w_{26} & 0 & w_{28} \\ w_{31} & 0 & 1 & w_{34} & w_{35} & 0 & w_{37} & 0 \\ w_{41} & 0 & w_{43} & 1 & 0 & 0 & 0 & 0 \\ 0 & 0 & 0 & 0 & 1 & 0 & w_{57} & 0 \\ 0 & 0 & w_{63} & w_{64} & w_{65} & 1 & 0 & w_{68} \\ 0 & 0 & w_{73} & 0 & 0 & 0 & 1 & w_{78} \\ 0 & w_{82} & 0 & 0 & 0 & w_{86} & w_{87} & 1 \end{bmatrix}$$

The values of the FCN nodes of FCN, can be extracted from the following equations:

$$A_i(k) = f\Big(\sum_{j\neq i}^{j=1} w_{ij}A_j(k-1) + A_i(k-1)\Big) \qquad (12)$$

Where $A_i(k)$ and $A_i(k-1)$ are the values of concept C_i at discrete time k and $k-1$ respectively, while concept C_j at discrete time $k-1$ has a value of $A_j(k-1)$. w_{ij} is the weight in the interval $[-1\ldots1]$, f is a squashing function: $f = 1/(1+e^{-x})$.

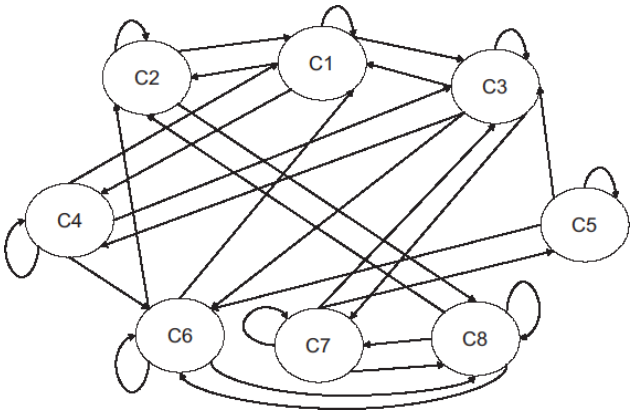

FIGURE 7. A simple fuzzy cognitive map/network.

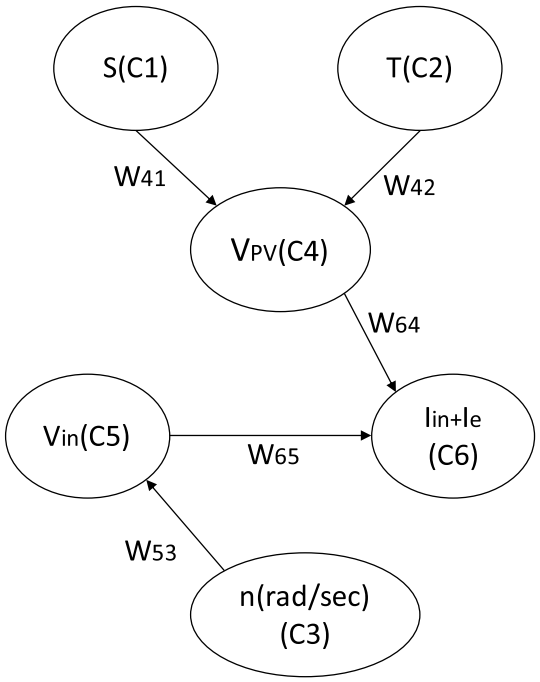

FIGURE 8. An FCN designed for speed motor control powered from PVs.

And for the steady state nodes the correction equation is:

$$A_j^{FCN}(k) = A_j^{system}(k) \tag{13}$$

where $A_j^{system}(k)$ is the node's value, derived from the physical system at discrete time k.

B. THE COGNITIVE GRAPH FOR THE PROJECT

The graph shown in Fig. 8 represents the speed control for the DC motor powered by a photovoltaic system, while having a Maximum Power Point Tracking capability. The graph consists of 6 nodes, where nodes C1, C2 and C3 are calculated according to eq. 13 and nodes C4, C5, C6 are control nodes (and are calculated according to eq. 12). The control node C4 is used to regulate the output voltage of the PV array and the input voltage of the motor as well, in order to achieve the desired speed. Each graph node corresponds to several physical quantities of the PV array and the DC motor as indicated in Table 2:

TABLE 2. Physical quantities of nodes of fcn.

Node	Description	Range of values
C1	solar insolation	$[0...1] \rightarrow [0 \ldots 100]mW / cm^2$
C2	temperature	$[0...1] \rightarrow [-30....70]°C$
C3	desired speed	$[0...1] \rightarrow [15....55]rad$ / sec
C4	optimum V_{pv}	$[0...1] \rightarrow [0....25]Volt$
C5	optimum V_{in}	$[0...1] \rightarrow [60....0]Volt$
C6	optimum I_{in}	$[0...1] \rightarrow [0....2]Ampere$

The weight matrix for the FCN is:

$$W = \begin{bmatrix} 0 & 0 & 0 & 0 & 0 & 0 \\ 0 & 0 & 0 & 0 & 0 & 0 \\ 0 & 0 & 0 & 0 & 0 & 0 \\ w_{41} & w_{42} & 0 & 1 & 0 & 0 \\ 0 & 0 & w_{53} & 0 & 1 & 0 \\ 0 & 0 & 0 & w_{64} & w_{65} & 1 \end{bmatrix}$$

while the vector A for nodes values is:

$$A = \begin{bmatrix} A_1 & A_2 & A_3 & A_4 & A_5 & A_6 \end{bmatrix}^T$$

C. THE FUZZY COGNITIVE NETWORK APPROACH FOR THE SPEED MOTOR CONTROL

FCNs were introduced by the authors of this paper, in a previous work, to solve Fuzzy Cognitive Maps critical problems and mainly to be used as a control method in physical systems and in recognition applications. An FCN consists of:

- the graph that graphically depicts the physical system one wants to recognize and finally control,
- the mechanism for updating the FCN weights values, which receives feedback from the physical system and
- the knowledge storage industry resulting from the different functional situations of the physical system imprinted through the FCN weights.

The topology of the FCN chart is originally drawn from the knowledge of the physical system's experts and captures the various concepts or variables of the system. FCN has the ability to capture every different state of the physical system through its weight values as a unique balance of graph and nodes values by using the weight update mechanism. As a consequence of relating the various operating conditions to equally various weight sets, Boutalis *et al.* [28] introduced a fuzzy rule based framework in order to store the various compounds. A view of the physical system along with the FCN that describes it, is presented in Fig. 9. The desired values A^{des} of the nodes of the FCN, represent input and output of the system and at the same time are the imprinting of the characteristics of the physical system. A number of FCN parameters will force the FCN to converge to an equilibrium point, namely A^{eq}. To estimate the aforementioned FCN

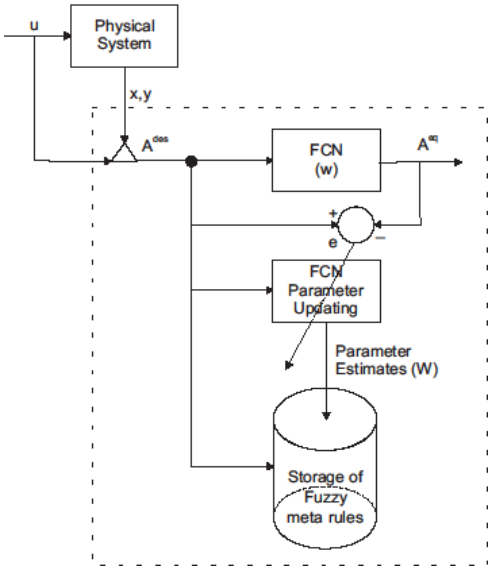

FIGURE 9. Interactive mode of FCN operation.

parameters we use the error between A^{des} and A^{eq}. Once the FCN weights are suitably adjusted, so they are now related to the current physical state of the physical system, they are stored in the form of unclear rules.

Fig 10 shows the flowchart of the proposed method where the designed FCN identifies the PV array-DC motor system under different climatic data. The FCN receives feedback from the physical system and from the Fuzzy Controller and sends control values to the DC / DC converter. The FCNs off-line identifier procedure of the physical system is performed in two stages, the weight updating procedure and the storage procedure is described below.

Step 1 (Weight Updating Procedure): This stage concerns the method of updating FCN's interconnection weights, taking into account training data. New weight values are calculated after a number of iterations leading the FCN to converge. Equations (12) and (13), referring to the calculation of the updated weights, are used by the FCN in each training iteration, in order to reach new equilibrium node values. Many updating algorithms for the parameters of FCNs were presented in the literature [29]. Authors introduced a weight updating algorithm [30], for the FCN's parameters:

$$\varepsilon_i(k) = \frac{f_i^{-1}(A_i^{des}) - w_i(k-1)A^{des}}{b + \left(A^{des}\right)^T A^{des}} \tag{14}$$

$$w_i(k) = w_i(k-1) + a\varepsilon_i(k)A^{des} \tag{15}$$

where $w_i(k)$ is the i-th row of matrix $W(k)$, A^{des} is a steady state vector, $f_i^{-1}(A_i^{des}) = w_i \cdot A^{des}$ is also a steady known vector. Parameters $a > 0$ and $b > 0$ are design parameters. Usually a=0.1 and b=0.1.

Step 2 (Building the Fuzzy Rule Database): The knowledge from the physical system modifies the weight values and consequently the values of the nodes according to the process of the previous step. Using equations (14) and (15) the FCN weights are updated so that they map the state of the physical

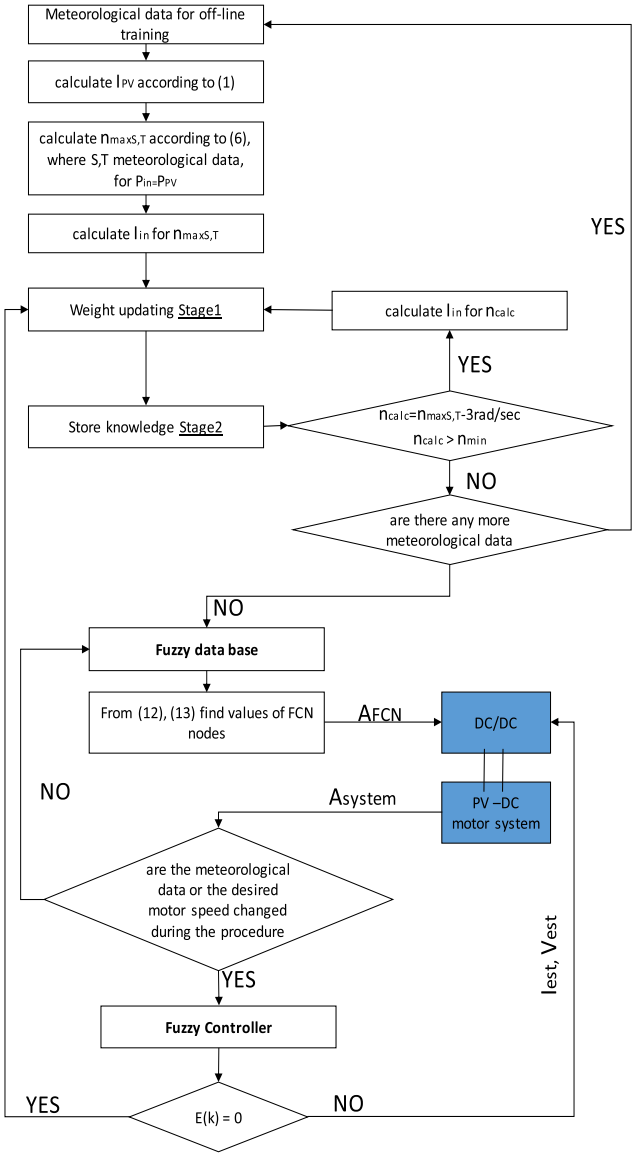

FIGURE 10. Simplified flowchart of the PV array-DC motor system controlled by FCNs.

system through a new equilibrium point. Given that, a weight matrix can generate new equilibrium values of the FCN node values. Each weight table now maps the current knowledge from the physical system. Boutalis *et al.* [28] introduced the way to store each new knowledge with the help of fuzzy if-then rules.

Let us make the assumption that there is a new data vector of the physical system, extracted after the FCN training, which then converges to the following weight matrix:

$$W = \begin{bmatrix} 0 & 0 & 0 & 0 & 0 & 0 \\ 0 & 0 & 0 & 0 & 0 & 0 \\ 0 & 0 & 0 & 0 & 0 & 0 \\ w_{41} & w_{42} & 0 & 1 & 0 & 0 \\ 0 & 0 & w_{53} & 0 & 1 & 0 \\ 0 & 0 & 0 & w_{64} & w_{65} & 1 \end{bmatrix}$$

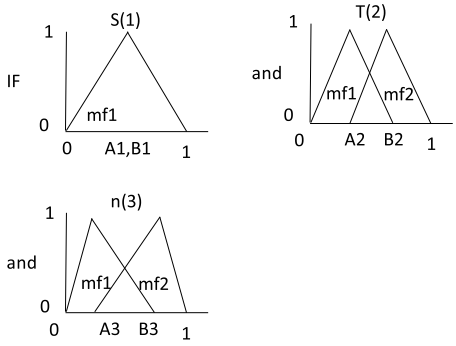

FIGURE 11. Left hand side (if part).

and concludes to an equilibrium state vector, according to eq. (12) and (13), which is:

$$A = \begin{bmatrix} A_1 & A_2 & A_3 & A_4 & A_5 & A_6 \end{bmatrix}^T$$

Suppose also that for a new weight matrix K,

$$K = \begin{bmatrix} 0 & 0 & 0 & 0 & 0 & 0 \\ 0 & 0 & 0 & 0 & 0 & 0 \\ 0 & 0 & 0 & 0 & 0 & 0 \\ k_{41} & k_{42} & 0 & 1 & 0 & 0 \\ 0 & 0 & k_{53} & 0 & 1 & 0 \\ 0 & 0 & 0 & k_{64} & k_{65} & 1 \end{bmatrix}$$

FCN nodes vector concludes to:

$$B = \begin{bmatrix} A_1 & B_2 & B_3 & B_4 & B_5 & B_6 \end{bmatrix}^T$$

The fuzzy rule database, is resolved as follows and is depicted in Figs 11, 12.

The aforementioned two different equilibrium situations are related to two rules respectively as follows:

Rule 1

if node 1 is mf1 and node 2 is mf1 and node 3 is mf1 **then** w41 is mf1 and w42 is mf1 and w53 is mf1 and w64 is mf1 and w65 is mf1

Rule 2

if node 1 is mf1 and node 2 is mf2 and node 3 is mf2 **then** w41 is mf2 and w42 is mf2 and w53 is mf2 and w64 is mf2 and w65 is mf2

In case a new triangular membership function occurs, having a difference from one already extracted value, which is greater than a specified threshold, then this new triangular function, is set to be a new training value. Fig. 13 depicts this procedure.

Control of the DC/DC Converter: The off-line trained FCN, is connected to the system PV array –DC motor according to Fig. 10. The FCN receives new operational data vectors from the PV array and the DC motor system. Once the Fuzzy controller error is set to zero, i.e. the input / output power of the DC / DC converter is set to the correct value, so that the PV array operates at maximum power, then these new maximum power operation point of the PV array sets a new equilibrium vector point to the FCN, which is used for further training.

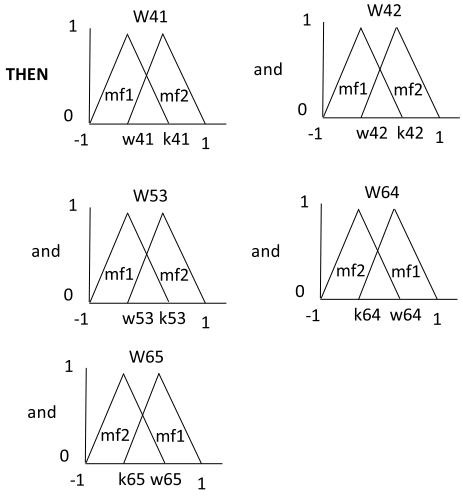

FIGURE 12. Right hand side (then part).

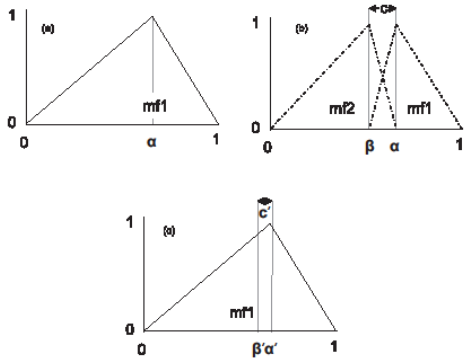

FIGURE 13. Creating new membership function. (a) Already encountered membership function, (b) $c >$ predefined threshold (new triangular created) and (c) $c <$ predefined threshold (no new triangular).

If there is any change in meteorological operational characteristics before the error E(k) of the Fuzzy Controller is set to zero, then the new insolation and temperature values force the FCN to adjust the process by applying a new pertinent MPP voltage value.

VII. RESULTS

Solar insolation and temperature play the most important role in the maximum power extracted from a PV array. These two quantities can be measured through a pyranometer and a thermocouple, although these technique is not always the most suitable information for determining the operating point that yields the maximum power. The photovoltaic short-circuit current is used to extract the most appropriate information about efficient solar insolation and temperature as depicted in equations (1) to (5).

The constructed training data's for the FCN are building according to the following procedure:

We select values for the Irradiation S(C1) in the range 0 mW/cm^2 to 100 mW/cm^2 using a step of 5 mW/cm^2.

And for the Temperature T(C2) we select values in the range $-20\ ^\circ C$ to $60\ ^\circ C$ using a step of $5\ ^\circ C$.

These numerous combinations of data in cooperation with the model simulating the PV array lead to the calculation of the optimum current values (node C4). Also from eq. (6) and from the current I_{PV} (node C4) calculated before, we calculate the optimum motor voltage V_{in} (node C5) and current (node C6) applied to the maximum allowed speed n (node C3) for the Irradiation and Temperature used before.

As an example, suppose that $T_r = 25°C$ and $S = 60mW/cm^2$, then the maximum current and voltage of the PV array is $I_{PV} = 2.8$A and $V_{PV} = 15.3$V, which means that $W_{PV} = 42.84$W. From eq. (6) when $W_{in} = W_{PV} = 42.84$W then $V_{in} = 43$V and $I_{in} = 0.99$A while speed motor is equal to n=38.7rad/sec. Needless to say that I_e is equal to zero because the power of the PV is applied to the motor. The evaluated node 1-6 values are used to update the FCN weights as described in the training procedure (stage 1). That leads to the calculation of a new equilibrium point for any possible combination and the storage of the extracted knowledge is made as mentioned in stage 2 of the procedure. Next, we calculate V_{in} and I_{in} for n=38.7-3=35.7rad/sec (node C3) where V_{in} and I_{in} is the new values for nodes C5 and C6. These new values for nodes C3, C5 and C6 ($I_e = I_{PV} - I_{in}$) with the already applied values of nodes C1, C2, and C4 form a new equilibrium point, updating the weights of the FCN (stage 1). Stage 2 is coming next for this new equilibrium point. The procedure is finished when $n=n_{min} = 26.7$rad/sec.

The possible combinations are 1662 and for those combinations the FCN builds a fuzzy rule database where for nodes C1 and C2 exists 21 triangular fuzzy membership functions, for node C3 exists 172 mf's, for node C4 exists 24 mf's, and for nodes C5 and C6 exists 172 mf's. The fuzzy rule database also creates, 542 fuzzy if-then rules, to store the knowledge.

In order to integrate the FCN to the DC motor - PV array system, the training part of the algorithm gets the values of nodes 1 to 3, if the error $E(k)$ of the Fuzzy Controller is zero. Following that, the system, using the fuzzy rule database, depicts the appropriate weights values for expressing node 4-6 values. Eqs. (12) and (13) in combination with the previously calculated weights are used to calculate the new FCN equilibrium operational point which represents the optimum values of the PV current referring to the existing insolation and temperature levels obtained at the specific time interval and the pertinent DC motor voltage and current referring respectively to the predefined motor.

Next the FCN sends the control values to the DC/DC converter No1, where the optimum voltage is determined, which corresponds to the maximum power of the PV array and the optimal speed of the motor for the specified temperature and solar insolation levels at the specific time.

Using the trained FCN we manage to control the operation of the DC/DC converter under different climatic conditions. The procedure showed the effectiveness of the proposed algorithm. Fig 14 presents the theoretical speed of the working motor for $S = 60mW/cm^2$, $T_r = 25°C$ and the applied speed driven by the FCN. It is obvious that when the motor is driven to operate in lower speed than the optimal, which

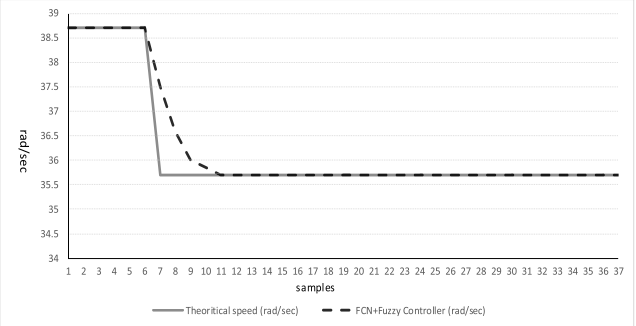

FIGURE 14. Sample vs Speed (rad/sec) of DC motor, *A. theoretical, B. proposed method for S=60mW/cm², T=25°C.*

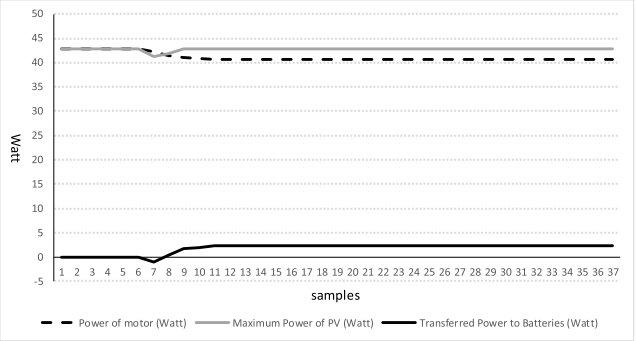

FIGURE 15. Sample vs Power applied to motor, Maximum power of PV array, transferred power to batteries for the applied speed of Fig. 14.

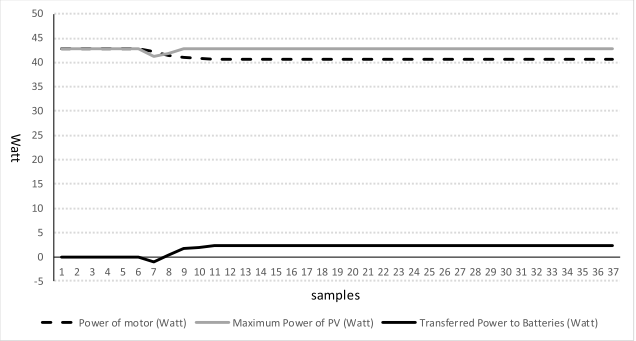

FIGURE 16. Sample vs desired speed, applied speed, irradiance S.

is the maximum one, the FCN rapidly, in only 3 samples (one sample is simulated as one second), changes the duty ratio of transistor S1 in order to achieve the desired voltage and current for the motor while at the same time transistor S2 starts to operate in order to transfer the extra energy from PV to the batteries, as it can be seen in Fig. 15.

Fig. 16 presents the desired speed of the motor, the applied speed of the motor and the irradiance. As the simulation starts the current climatic conditions are $S = 70mW/cm^2$, $T_r = 25°C$ while motor speed is 41.4 rad/sec. In sample 5 the desired speed is now 37.5 rad/sec where the FCN reaches it by controlling transistor S1 in only 2 samples. In sample 9 the applied irradiance changes to $S = 40mW/cm^2$,

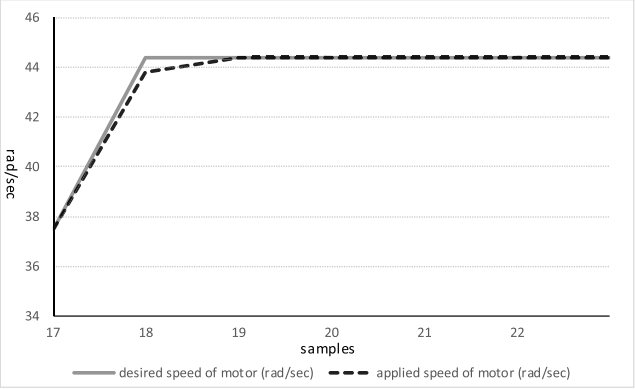

FIGURE 17. Sample vs desired speed and applied speed for samples 17 to 22 of Fig. 16.

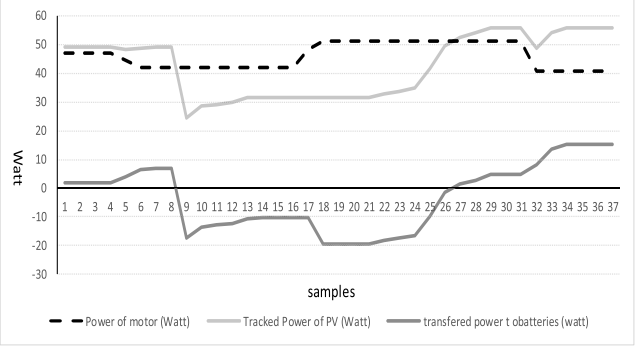

FIGURE 18. Sample vs Power applied to motor, tracked power of PV array, transferred power to batteries for the applied speed of simulation of Fig. 16.

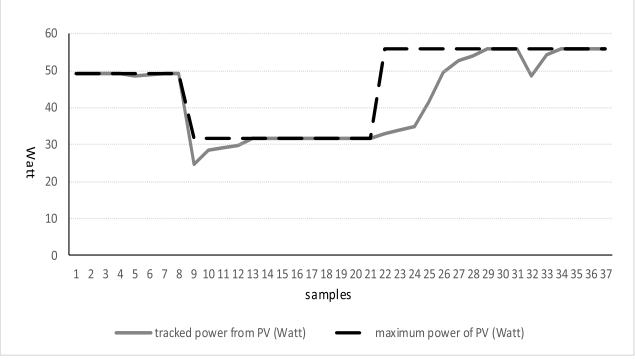

FIGURE 19. Sample vs maximum power of PV array, tracked power of PV from FCN controller of simulation of Fig. 16.

where the FCN starts to change the duty ratio, in close cooperation with the Fuzzy Controller, in order to find the new maximum power point of the PV array which is now 31.8Watt. The applied speed remains at 37.5rad/sec. This change in irradiance results to a new equilibrium point for the FCN. FCN reaches the new maximum power of the PV in only 6 samples, where the motor speed is changing from 37.5rad/sec to 36.9rad/sec for only 2 samples until it reaches again the desired value. At sample 17 the desired motor speed is changing from 37.5rad/sec to 44.4rad/sec, where the FCN reacts in only 2 samples to achieve the desired speed value. A more detailed view of the simulation from sample 17 to sample 22 can be seen in Fig. 17. At sample 22 the irradiance changes from $S = 40mW/cm^2$ to $S = 80mW/cm^2$ where the FCN reacts in 8 samples to achieve the maximum power of the PV by keeping the speed of the motor to the desired speed of 44.4rad/sec. A more detailed view of the reaction of the FCN controller as it concerns the tracked power of the PV array the applied and tracked power from the batteries, it can be seen in Figs. 18 and 19. In sample 32 the desired speed is now 35.7rad/sec (see fig. 16) where one could see a drop for 4 samples in the tracked power from the PV until the FCN could reach the maximum power for the PV and achieve the desired speed for the motor in only 3 samples.

VIII. CONCLUSION

In the present study a new algorithm-method for controlling a DC shunt motor's speed using FCN was presented. A new connection topology from the PV to the DC motor was proposed, where a battery was used so that the energy that PV delivers to the system motor-battery is always in the maximum point and the energy that the motor demands is always available from the system PV-battery. The problem that had to be solved algorithmically was complicated and unclear because both the PV and the motor had different characteristic curves of operation which through a DC / DC converter and a control algorithm had to be combined so that both PV delivers the maximum power and the motor rotates at the desired values. The new connection topology as well as the new algorithm showed particular characteristics of adaptation to the desired values of both motor speed and the maximum transferred energy from the PV.

REFERENCES

[1] S. M. Alghuwainem, "Steady-state performance of DC motors supplied from photovoltaic generators with step-up converter," *IEEE Trans. Energy Convers.*, vol. 7, no. 2, pp. 267–272, Jun. 1992.
[2] S. M. Alghuwainem, "Speed control of a PV powered DC motor driving a self-excited 3-phase induction generator for maximum utilization efficiency," *IEEE Trans. Energy Convers.*, vol. 11, no. 4, pp. 768–773, Dec. 1996.
[3] S. S. Chandel, M. N. Naik, and R. Chandel, "Review of performance studies of direct coupled photovoltaic water pumping systems and case study," *Renew. Sustain. Energy Rev.*, vol. 76, pp. 163–175, Sep. 2017.
[4] J. Appelbaum, "Starting and steady-state characteristics of DC motors powered by solar cell generators," *IEEE Trans. Energy Convers.*, vol. EC-1, no. 1, pp. 17–25, Mar. 1986.
[5] G. Dileep and S. N. Singh, "Selection of non-isolated DC-DC converters for solar photovoltaic system," *Renew. Sustain. Energy Rev.*, vol. 76, pp. 1230–1247, Sep. 2017.
[6] M. M. Saied, "Matching of DC motors to photovoltaic generators for maximum daily gross mechanical energy," *IEEE Trans. Energy Convers.*, vol. EC-3, no. 3, pp. 465–472, Sep. 1988.
[7] J. Appelbaum, "The operation of loads powered by separate sources or by a common source of solar cells," *IEEE Trans. Energy Convers.*, vol. 4, no. 3, pp. 351–357, Sep. 1989.
[8] M. A. Elgendy, B. Zahawi, and D. J. Atkinson, "Comparison of directly connected and constant voltage controlled photovoltaic pumping systems," *IEEE Trans. Sustain. Energy*, vol. 1, no. 3, pp. 184–192, Oct. 2010.
[9] R. Kumar and B. Singh, "BLDC motor-driven solar PV array-fed water pumping system employing zeta converter," *IEEE Trans. Ind. Appl.*, vol. 52, no. 3, pp. 2315–2322, May 2016.

[10] S. Sashidhar and B. G. Fernandes, "A novel ferrite SMDS spoke-type BLDC motor for PV bore-well submersible water pumps," *IEEE Trans. Ind. Electron.*, vol. 64, no. 1, pp. 104–114, Jan. 2017.
[11] R. Kumar and B. Singh, "Single stage solar PV fed brushless DC motor driven water pump," *IEEE J. Emerg. Sel. Topics Circuits Syst.*, vol. 5, no. 3, pp. 1377–1385, Sep. 2017.
[12] Z. Zinger and A. Braunstein, "Dynamic matching of a solar-electrical (photovoltaic) system an estimation of the minimum requiremnts on the matching system," *IEEE Trans. Power App. Syst.*, vol. PAT-100, no. 3, pp. 1189–1192, Mar. 1981.
[13] J. J. Schoeman and J. D. Van Wyk, "A simplified maximal power controller for terrestrial photovoltaic panel arrays," in *Proc. IEEE Power Electron. Specialist Conf. (PESC)*, Jun. 1982, pp. 361–367.
[14] S. M. Alghuwainem, "Application of a DC chopper to maximize utilization of solar-cell generators," in *Proc. IEEE/PES Winter Meeting*, New York, NY, USA, Feb. 1991, paper 91 WM 145-3 EC.
[15] M. A. Elgendy, B. Zahawi, and D. J. Atkinson, "Assessment of the incremental conductance maximum power point tracking algorithm," *IEEE Trans. Sustain. Energy*, vol. 4, no. 1, pp. 108–117, Jan. 2013.
[16] P. Karthika, M. A. Basha, P. Ayyappan, K. C. Sidharthan, and R. V. Rajakumar, "PV based speed control of DC motor using interleaved boost converter with SIC MOSFET and fuzzy logic controller," in *Proc. Int. Conf. Commun. Signal Process.*, Melmaruvathur, India, Apr. 2016, pp. 1826–1830.
[17] C.-Y. Won, D.-H. Kim, S.-C. Kim, W.-S. Kim, and H.-S. Kim, "A new maximum power point tracker of photovoltaic arrays using fuzzy controller," in *Proc. 25th Annu. IEEE Power Electron. Specialists Conf. (PESC)*, vol. 1. Jun. 1994, pp. 396–403.
[18] M. G. Simoes and N. N. Franceschetti, "Fuzzy optimization based control of a solar array," *IEE Proc. Electr. Power Appl.*, vol. 146, no. 5, pp. 552–558, Sep. 1999.
[19] I. H. Altas and A. M. Sharaf, "A novel on-line MPP search algorithm for PV arrays," *IEEE Trans. Energy Convers.*, vol. 11, no. 4, pp. 748–754, Dec. 1996.
[20] H. Matsukawa, K. Koshiishi, H. Koizumi, K. Kurokawa, M. Hamada, and L. Bo, "Dynamic evaluation of maximum power point tracking operation with PV array simulator," *Solar Energy Mater., Solar Cells*, vol. 75, nos. 3–4, pp. 537–546, 2003.
[21] M. A. S. Masoum, S. M. M. Badejani, and E. F. Fuchs, "Microprocessor-controlled new class of optimal battery chargers for photovoltaic applications," *IEEE Trans. Energy Convers.*, vol. 19, no. 3, pp. 599–606, Sep. 2004.
[22] L. T. Kottas, S. Y. Boutalis, and D. A. Karlis, "New maximum power point tracker for PV arrays using fuzzy controller in close cooperation with fuzzy cognitive networks," *IEEE Trans. Energy Convers.*, vol. 21, no. 3, pp. 793–803, Sep. 2006.
[23] A. D. Karlis, T. L. Kottas, and Y. S. Boutalis, "A novel maximum power point tracking method for PV systems using fuzzy cognitive networks (FCN)," *Electr. Power Syst. Res.*, vol. 77, nos. 3–4, pp. 315–327, Mar. 2007.
[24] T. Kottas, Y. Boutalis, and M. Christodoulou, "A new method for weight updating in fuzzy cognitive maps using system feedback," in *Proc. 2nd Int. Conf. Informat. Control, Autom. Robot.*, Barcelona, Spain, Sep. 2005, pp. 202–209.
[25] C. Hua and C. Shen, "Study of maximum power tracking techniques and control of DC/DC converters for photovoltaic power system," in *Proc. 29th Annu. IEEE Power Electron. Specialists Conf.*, 1998, pp. 86–93.
[26] C. Lee, "Fuzzy logic in control systems: Fuzzy logic controller. I," *IEEE Trans. Syst., Man, Cybern., Syst.*, vol. 20, no. 2, pp. 404–435, Mar./Apr. 1990.
[27] T. L. Kottas, Y. S. Boutalis, and M. A. Christodoulou, "Fuzzy cognitive networks: A general framework," in *Intelligent Decision Technologies*, vol. 1. 2007, pp. 183–196.
[28] Y. Boutalis, T. Kottas, B. Mertzios, and M. Christodoulou, "A fuzzy rule based approach for storing the knowledge acquired from dynamical FCMs," in *Proc. 5th Int. Conf. Technol. Autom. (ICTA)*, Thessalonica, Greece, Oct. 2005, pp. 119–124.
[29] I. Elpiniki Papageorgiou, "Learning algorithms for fuzzy cognitive maps—A review study," *IEEE Trans. Syst., Man, Cybern. C, Appl. Rev.*, vol. 42, no. 2, pp. 150–163, Mar. 2012.
[30] Y. Boutalis, T. L. Kottas, and M. Christodoulou, "Adaptive estimation of fuzzy cognitive maps with proven stability and parameter convergence," *IEEE Trans. Fuzzy Syst.*, vol. 17, no. 4, pp. 874–889, Aug. 2009.

THODORIS L. KOTTAS received the Dipl.-Eng., M.Sc., and Ph.D. degrees from the Electrical and Computer Engineering Department, Democritus University of Thrace, Greece, in 2003, 2005, and 2017, respectively. He is a Visitor Teacher with the Electrical Engineer Department, Technological Educational Institute of Western Macedonia, Kozani, Greece. His research interests include intelligent modeling and control techniques with applications in power production and conversion.

ATHANASIOS D. KARLIS (M'00–SM'12) received the Dipl.-Eng. and Ph.D. degrees from the Electrical and Computer Engineering Department, Aristotle University of Thessaloniki, Greece, in 1991 and 1996, respectively. He is currently an Associate Professor with the Department of Electrical and Computer Engineering, Democritus University of Thrace, Greece. His research interests include electrical machines and drives, renewable energy sources, and electrical power systems. He served as a member of the Board of Directors of the Hellenic Institute of Electric Vehicles, for two years. He is also the Founder and Advisor of the Democritus University of Thrace IEEE IAS SBC and a Chair of the IEEE IES/IAS/PELS Joint Chapter (Greece Section). He received the IEEE Outstanding Branch Chapter Advisor Award for 2015 and the Outstanding IEEE IAS Student Branch Chapter Advisor Award for 2016.

YIANNIS S. BOUTALIS received the Dipl.-Eng. from the Democritus University of Thrace (DUTH), Greece, in 1983, and the Ph.D. degree in electrical and computer engineering from the Computer Science Division of National Technical University of Athens, Greece, in 1988. He served as an Assistant Visiting Professor with the University of Thessaly, Greece, and as a Visiting Professor with the Hellenic Air Force Academy of General Staff, Air Forces of Greece. In the last years, he has been several times a Visiting Scholar with the Friedrich-Alexander University of Erlangen, Nuremberg, Germany, and the Chair of Automatic Control. Since 1996, he has been serving as a Faculty Member with the Department of Electrical and Computer Engineering, DUTH, where he is currently a Professor and the Director of the Laboratory of Automatic Control Systems & Robotics. He also served as a Researcher with the Institute of Language and Speech Processing, Greece, and a Managing Director of the R&D SME Ideatech S.A, Greece, specializing in pattern recognition and signal processing applications. His current research interests are focused in the development of computational intelligence techniques with applications in control, pattern recognition, signal, and image processing problems.